Article citation info:
KARPIŃSKI, P., PIETRYKOWSKI, K., GRABOWSKI, Ł. Turbocharging the aircraft two-stroke diesel engine. *Combustion Engines*. 2019, **178**(3), 112-116. DOI: 10.19206/CE-2019-319

Paweł KARPIŃSKI
Konrad PIETRYKOWSKI
Łukasz GRABOWSKI

CE-2019-319

Turbocharging the aircraft two-stroke diesel engine

The power and efficiency of a two-stroke engine strongly depends on the efficiency of the scavenging process which consists in removing the rest of the exhaust gases from the cylinder and filling it with a fresh charge. The quality of the charge exchange process is significantly influenced by the construction of the intake system. The paper presents a zero-dimensional model of the aircraft two-stroke opposed-piston diesel engine with two variants of the intake system: with a mechanical compressor and a turbocharger connected in series with a mechanical compressor. Simulation studies of the developed cases were carried out in the AVL BOOST software. For the defined engine operating points, its performance was compared for different designs of the intake system. It was confirmed that the use of a turbocharger with a mechanical compressor extends the range of operating at high altitudes.

Key words: *aircraft engine, two-stroke engine, diesel engine, turbocharger, supercharger*

1. Introduction

Two-stroke opposed piston engines (OP2S) have a simpler design, better balance and competitive performance when compared to four-stroke inline engines [1]. The paper [2] presents thermodynamic benefits of the construction of two-stroke engines with opposed pistons. In recent years, numerous research works have been carried out on such engines that differ in the construction of the crank-piston system, e.g. the works [3] and [4] analyzed injection and scavenging processes in OP2S engines.

In two-stroke opposed piston engines, an external device as a mechanical compressor or turbocharger is necessary to carry out the load exchange process. It is also possible to use a combination of these devices. Such a solution is presented in the paper [5] where the blower operates under low load and low speed conditions, while the turbocharger is the main device to exchange a charge. The work [6] discusses the investigations on the influence of selected blower and turbocharger configurations on the performance of a two-stroke diesel engine. The system of two turbochargers in a series system was also analyzed. The analysis of a similar configuration and the general turbocharging analysis of the automotive two-stroke engine were presented in the paper [7]. Research was also carried out on a supercharged two-stroke SI engine with uniflow scavenging under high altitude conditions [8]. In the paper [9], the performance of the turbocharged two-stroke diesel engine was analyzed, focusing on thermal efficiency, load and specific fuel consumption.

As flight altitude increases, volumetric efficiency and thus engine power decreases. An additional turbocharger in the aircraft engine enables the required power to be maintained in high altitude flight as well as a momentary increase in power during take-off and climbing. The benefits of turbocharging a two-stroke diesel engine are presented in the paper [10].

A quick, effective and low-cost method of testing engine's operating parameters are tests using mathematical models. This approach is discussed in the work [11] where a zero-dimensional engine model is presented and the influence of variable compression ratio on engine performance is examined.

The paper analyzes how a turbocharger in a two-stroke opposed piston aircraft diesel engine influences this engine performance at four defined operating points. The created engine model enabled us to compare the selected operating parameters with these calculated for the engine variant equipped only with the mechanical compressor.

2. Engine model

The research object was a three-cylinder two-stroke opposed piston aircraft diesel engine at the design stage. The basic engine parameters are shown in Table 1.

Table 1. Basic technical parameters of the tested engine

Maximum power	100 kW
Engine speed	4200 rpm
Number of cylinders	3
Bore	65.5 mm
Stroke	72 mm
Compression ratio	22:1
Scavenging	Uniflow

In order to perform simulation tests in the AVL BOOST software, a zero-dimensional model of the tested engine in two variants was developed (Fig. 1): with a mechanical compressor (Fig. 2) and a turbine connected in series with a smaller mechanical compressor (Fig. 3). Both variants have an air intercooler at the end of the inlet duct. The Vibe model was adopted as a combustion model and the Woschni model as a heat exchange model.

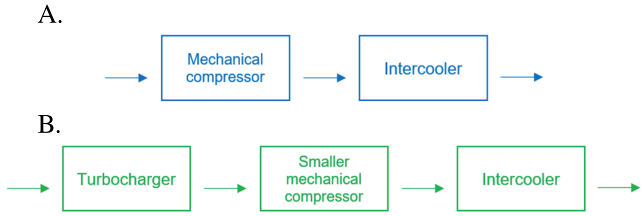

Fig. 1. Analyzed variants of the intake system

In variant A, the Eaton TVS R900 compressor operating map developed by the manufacturer was implemented in the model. The map is defining the efficiency and power consumed by the device as a function of the compression ratio and mass flow of air.

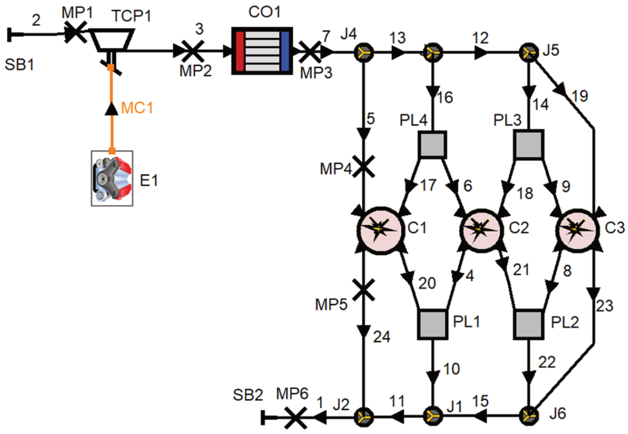

Fig. 2. Model of the engine with the Eaton TVS R900 mechanical compressor

Variant B implemented the Garrett GT-2560R turbocharger maps which presented compressor efficiency as a function of compression and mass air flow as well as mass flow through the turbine as a function of the compression ratio. In the series connection, a smaller Eaton TVS R410 mechanical compressor was used whose operating map was introduced into the model.

Additional calculations were performed for the variant with a changed order of devices, i.e. turbocharger–mechanical compressor–intercooler. This case was rejected after the initial calculations. The Eaton TVS R410 compressor did not provide stable operation in subsequent computational cycles. The obtained power for a cruising power point at an altitude of 4600 m was 62 kW and was 11 kW lower than the reference value for this case.

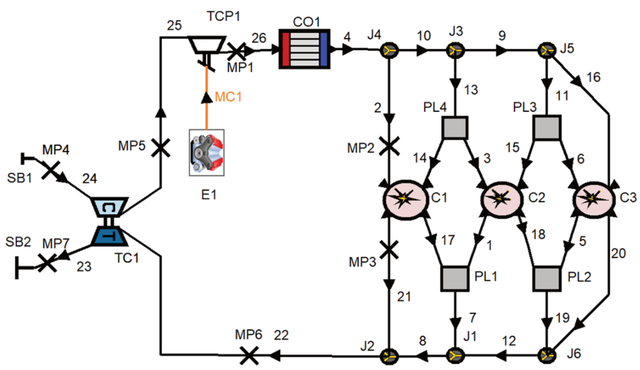

Fig. 3. Model of the engine with the Garrett GT-2560R turbocharger connected in series with the Eaton TVS R410 mechanical compressor

The so-called offset, i.e. a phase shift between the engine crankshafts, was defined in the model. This shift allows improving the scavenging process in a two-stroke engine with uniflow scavenging. The offset was implemented by changing the characteristics of the inlet and outlet windows in the cylinder settings. In the considered case, the crankshaft on the side of the outlet windows is ahead of the crankshaft on the side of the intake windows by 14°.

The calculations were carried out for four defined operating points: take-off power, continuous maximum power, cruising power at 0 m and cruising power at 4600 m (15000 ft). The operating points were characterized by engine speed, air-to-fuel ratio (AFR) and start of combustion angle (SoC). The set-ups of operating points for the first and second variants are shown in Tables 2 and 3, respectively.

Table 2. Defined operating points for the variant with the Eaton TVS R900 mechanical compressor

Operating point	Power [kW]	Engine speed [rpm]	AFR [–]	SoC [°]	H [m]
Take-off power	100	4200	22	+3.5°	0
Maximum continuous power	86	4000	24	–2.5°	0
Cruising power, H = 0 m	73	3800	27	0°	0
Cruising power, H = 4600 m	73	3800	22	–3.5°	4600

Table 3. Defined operating points for the variant with the Garrett GT-2560R turbocharger and the Eaton TVS R410 mechanical compressor

Operating point	Power [kW]	Engine speed [rpm]	AFR [–]	SoC [°]	H [m]	WV [%]
Take-off power	100	4200	22	+2.5°	0	0.53
Maximum continuous power	86	4000	24	–0.5°	0	0.53
Cruising power, H = 0 m	73	3800	27	–1.0°	0	0.57
Cruising power, H = 4600 m	73	3800	22	–2.0°	4600	0.76

The additional parameter for the variant with a turbocharger was the wastegate valve opening coefficient (WV). This parameter controls the power generated by the engine. The SoC angle value for each case was changed so that the maximum cylinder pressure did not exceed 13 MPa. The adopted value results from the design assumptions and strength limits for the tested engine.

3. Results and discussion

The simulation calculations enabled us to obtain the values of selected engine operation parameters for the two variants. These values i.e. the specific fuel consumption, the compressor power, the effective pressure and the pressure in the intake manifold before the cylinders were compared with each other.

For the case of a cruising power at an altitude of 4600 m for the variant with the Eaton TVS R900 compressor, the engine generated the power of 59 kW so the assumed power value of 73 kW was not obtained. For the case with a turbocharger, the defined power was obtained by closing the by-pass valve.

Figure 4 shows the specific fuel consumption for the considered operating points for the analyzed cases. For the variant with a turbocharger, fuel consumption was reduced by up to 12%. For continuous power, specific fuel consumption decreased from 248.3 g/kWh to 217.4 g/kWh. For a cruising power at an altitude of 4600 m, a slight increase in specific fuel consumption up to 223 g/kWh was recorded.

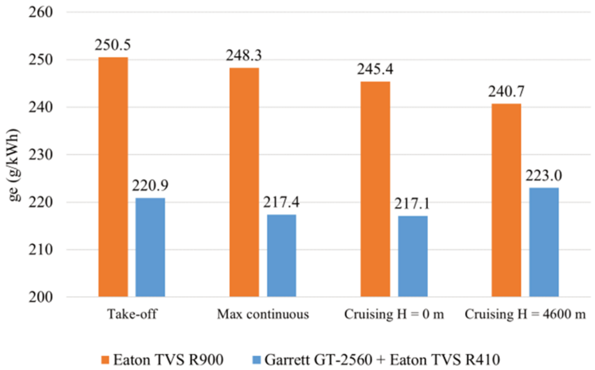

Fig. 4. Comparison of the specific fuel consumption for two analyzed variants

The power consumed by the compressor for the considered cases is shown in Fig. 5. For the case with the Eaton TVS R900 compressor, the power consumed by the compressor decreased with the decreasing power generated by the engine. For the variant with a turbocharger, the consumed power was reduced by more than half for the take-off power operating point and the continuous maximum power point. For cruising power at 4600 m, this value decreased by 32%.

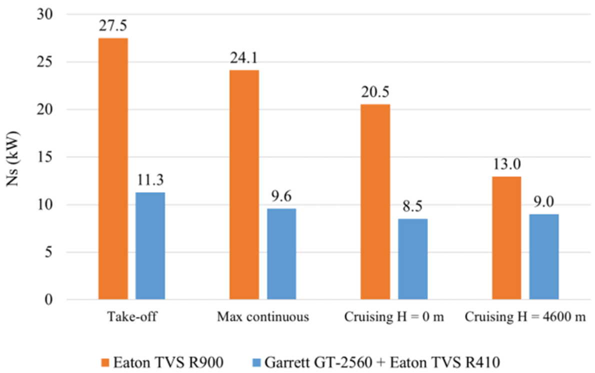

Fig. 5. Comparison of the compressor power for two analyzed variants

The value of the average effective pressure for the variant with the turbocharger was lower by 10–12% than for the variant with the mechanical compressor only. However, for both cases, the same power was obtained due to the fact that the turbocharger improved the filling of the cylinder with fresh air. In the case of the variant with the turbocharger, the increase in altitude did not cause a drop in the effective pressure. A summary of the effective pressure values for the studied cases was shown in Fig. 6.

Intake manifold pressure (Fig. 7) for the variant with a mechanical compressor only was higher by about 40% compared to the variant with the turbocharger. For the case of cruising power at an altitude of 4600 m, the pressure for the variant with the turbocharger was 138 kPa and was 20% higher compared to the variant with the Eaton TVS R900 compressor.

Figure 8 shows a map of the Eaton TVS R900 mechanical compressor with operating points. All points are within the efficiency range of 62-67%. The highest efficiency was obtained for the cruising power at H = 0 m. As the height increases, the operating point shifts to the left towards the smaller mass flow on the map and for the height H = 4600 m, the efficiency is equal to 62%.

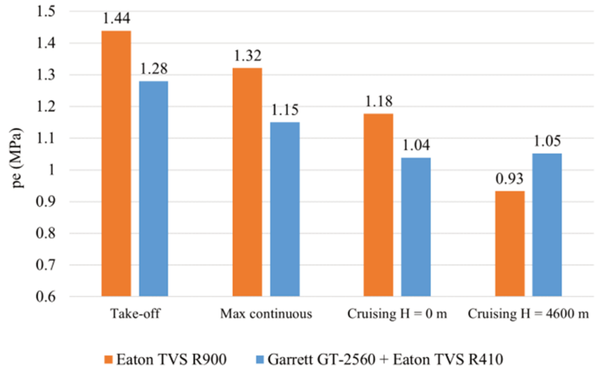

Fig. 6. Comparison of the effective pressure for two analyzed variants

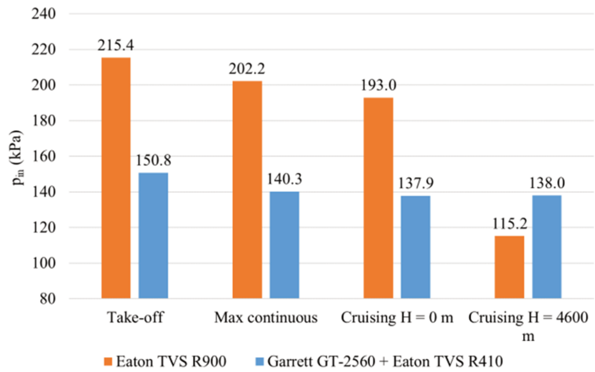

Fig. 7. Comparison of inlet manifold pressure for two analyzed variants

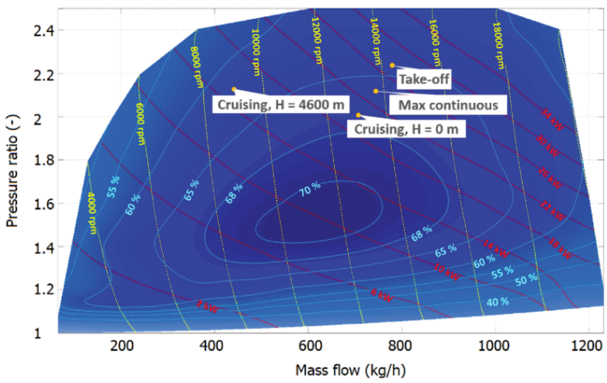

Fig. 8. Eaton TVS R900 compressor map with calculated operating points [12]

The determined operating points for the Eaton TVS R410 compressor are shown in Fig. 9. The efficiency achieved varied in the range of 65-66%. The highest efficiency equal to 66% was obtained for the cruising power point at H = 4600 m. For the cruising power at H = 0 m, the efficiency was equal to 65%. As the height increases, the operating points move on the map upwards through the area with the highest efficiency of the compressor.

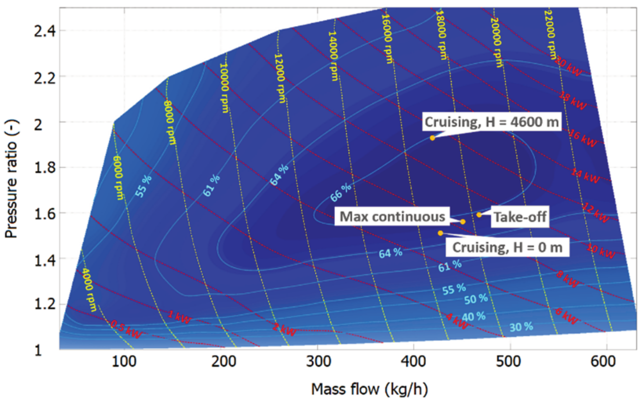

Fig. 9. Eaton TVS R410 compressor map with calculated operating points [13]

The map of the Garrett GT-2560R turbocharger is shown in Fig. 10. The three points: take-off power, maximum continuous power and cruising power at H = 0 m are below the 55% efficiency. With the increase of the height, the operating point is moved upwards on the map, achieving its efficiency about 70% for the cruising power at H = 4600 m.

4. Conclusions

The paper presents the results of research on the model of two-stroke opposed piston aircraft diesel engine. The research investigated the impact of a turbocharger with a mechanical compressor on engine performance. The results obtained for this case were compared to the results for an engine equipped with a mechanical compressor only.

Engine performance was significantly improved by means of a turbocharger with a smaller mechanical compressor. The specific fuel consumption decreased by 12%, the power consumed by the compressor for the maximum continuous power dropped by 14 kW, and the range of engine operation at high altitude increased. In the case of an R900 compressor, it was impossible to achieve the assumed value of a cruising power of 73 kW at 4600 m. By the application of the turbocharger, the defined power was obtained and the intake manifold pressure at high altitudes remained constant compared to the cruising power at H = 0 m.

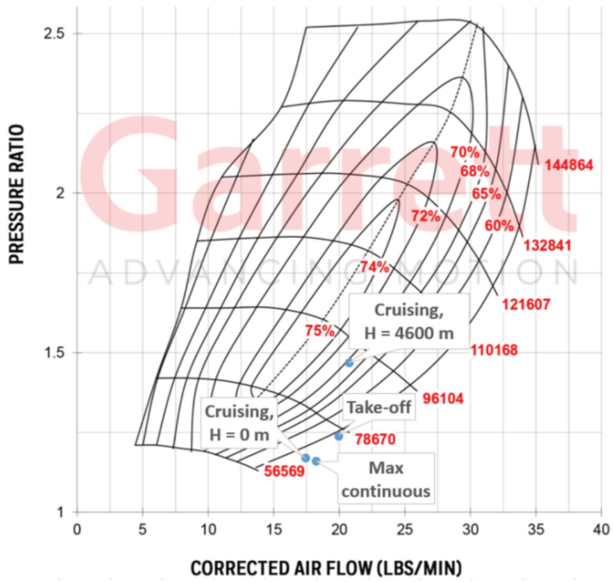

Fig. 10. Garrett GT-2560R turbocharger map with calculated operating points [14]

A turbocharger–mechanical compressor layout, besides improving engine performance, is capable of improving aircraft safety. If one of the devices fails, the other is able to provide fresh air supply to cylinders so it is possible to obtain some power to keep engine and key auxiliary devices temporarily operating.

Acknowledgements

This work has been performed in the cooperation with The Construction Office of WSK "PZL-KALISZ" S.A." and is part of Grant Agreement No. POIR.01.02.00-00-0002/15 financed by the Polish National Centre for Research and Development.

Nomenclature

AFR air to fuel ratio
SI spark ignition
SoC start of combustion
WV wastegate valve opening coefficient

Bibliography

[1] PIRAULT, J.P., FLINT, M. Opposed piston engines: evolution, use, and future applications. *SAE International*. 2010.

[2] HEROLD, R.E., WAHL, M.H., REGNER, G. et al. Thermodynamic benefits of opposed-piston two-stroke engines. *SAE Technical Paper*. 2011, 2011-01-2216. DOI:10.4271/2011-01-2216

[3] ZHANG, L., SU, T., ZHANG, Y. et al. Numerical investigation of the effects of split injection strategies on combustion and emission in an opposed-piston, opposed-cylinder (OPOC) two-stroke diesel engine. *Energies*. 2017, **10**(5), 684. DOI:10.3390/en10050684

[4] LIU, Y., ZHANG, F., ZHAO, Z. et al. The effects of pressure difference on opposed piston two stroke diesel engine scavenging process. *Energy Procedia*. 2017, **142**, 1172-1178. DOI:10.1016/j.egypro.2017.12.374

[5] BLAIR, G.P. Design and simulation of two-stroke engines. *Society of Automotive Engineers*. 1996.

[6] TIMONEY, S.G. High pressure turbocharging of two-stroke engines. *SAE Transactions*, 1969, 2401-2412. DOI:10.4271/690747

[7] TRYHORN, D.W. Turbocharging the automotive two-stroke cycle engine. *Proceedings of the Institution of Mechanical Engineers*. 1965, **180**(14), 75-84. DOI:10.1243/PIME_CONF_1965_180_387_02

[8] LAND, M.L., CARAMEROS, A. Turbocharged two-stroke-cycle gas engines. *Journal of Engineering for Power*. 1965, **87**(4), 421-438. DOI:10.1115/1.3678291

[9] GUNES, U., UST, Y., KARAKURT, A.S. Performance analysis of turbocharged 2-stroke diesel engine.

[10] FINDLAY, A., HARKER, N., DEN BRAVEN, K.R. Brake specific fuel consumption and power advantages for a turbo-

charged two-stroke direct-injected engine. *International Mechanical Engineering Congress and Exposition*.2008, 269-279. DOI:10.1115/IMECE2008-68371
[11] ALQAHTANI, A., WYSZYNSKI, M.L., MAZURO, P., XU, H. Evaluation of the effect of variable compression ratios performance on opposed piston 2-stroke engine. *Combustion Engines*. 2017, **171**(4), 97-106.
[12] Eaton TVS R900 supercharger specification https://www.eaton.com/us/en-us/catalog/engine-solutions/tvs-r900.specifications.html
[13] Eaton TVS R410 supercharger specification, https://www.eaton.com/us/en-us/catalog/engine-solutions/tvs-r410.specifications.html
[14] Garrett GT-2560R turbocharger specification, https://www.garrettmotion.com/racing-and-performance/performance-catalog/turbo/gt2560r/

Paweł Karpiński, MEng. – Faculty of Mechanical Engineering, Lublin University of Technology.
e-mail: *pawel.karpinski@pollub.edu.pl*

Grabowski Łukasz, DEng. – Faculty of Mechanical Engineering, the Lublin University of Technology.
e-mail: *l.grabowski@pollub.pl*

Konrad Pietrykowski, DEng. – Faculty of Mechanical Engineering, Lublin University of Technology.
e-mail: *k.pietrykowski@pollub.pl*